Deep learning

7.3. Denoising autoencoders

François Fleuret
https://fleuret.org/dlc/

Beside dimension reduction, autoencoders can capture dependencies between signal components to restore a degraded input.

In that case, we can ignore the encoder/decoder structure, and such a model

$$\phi : \mathcal{X} \to \mathcal{X}.$$

is referred to as a **denoising** autoencoder.

The goal is not anymore to optimize ϕ so that

$$\phi(X) \simeq X$$

but, given a perturbation $\tilde{X}$ of the signal X, to restore the signal, hence

$$\phi(\tilde{X}) \simeq X.$$

We can illustrate this notion in $2d$ with an additive Gaussian noise, and the quadratic loss, hence

$$\hat{w} = \operatorname*{argmin}_{w} \frac{1}{N} \sum_{n=1}^{N} \|x_n - \phi(x_n + \epsilon_n; w)\|^2 ,$$

where x_n are the data samples, and ϵ_n are Gaussian random noise vectors.

```
model = nn.Sequential(
    nn.Linear(2, 100),
    nn.ReLU(),
    nn.Linear(100, 2)
)

batch_size, nb_epochs = 100, 1000
optimizer = torch.optim.Adam(model.parameters(), lr = 1e-3)
mse = nn.MSELoss()

for e in range(nb_epochs):
    for input in data.split(batch_size):
        noise = input.new(input.size()).normal_(0, 0.1)
        output = model(input + noise)
        loss = mse(output, input)

        optimizer.zero_grad()
        loss.backward()
        optimizer.step()
```

Notes

We define a MLP `model` that goes from $\mathbb{R}^2$ to $\mathbb{R}^2$ and has 100 hidden units and the ReLU activation function.
For each minibatch, a centered Gaussian noise with standard deviation of 0.1 is added to the samples.
The loss is computed between the input sample without noise, and the output of the network on the noisy sample.

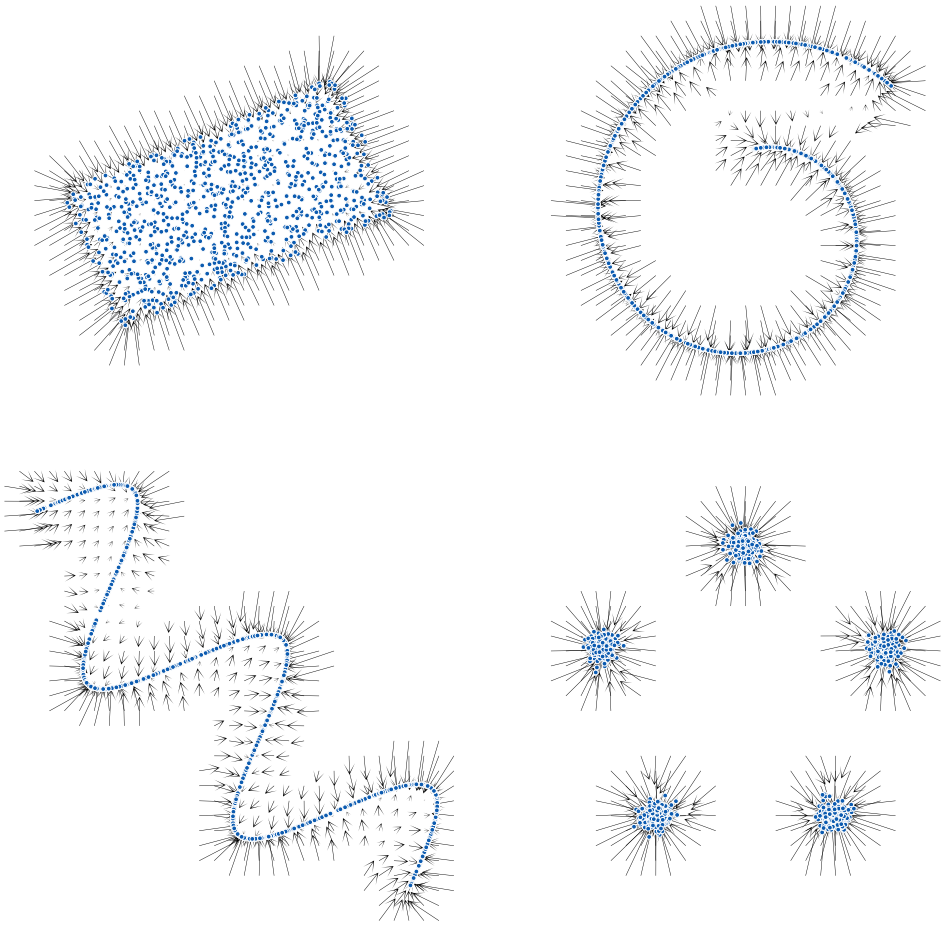

Notes

These pictures illustrate the denoising autoencoder ϕ of the previous slide on toy 2d examples. In each figure the blue dots are the training points sampled from μ_X.

The arrows are drawn by iterating over the points on a regular grid, and for every such point x not "too far" from the training data, drawing a arrow from x to $\phi(x)$.

We see that the autoencoder learned to take the points "back" to the [support of the] distribution. Points which are already in the [support of the] distribution, e.g. inside the rectangle, are not moved, and the resulting arrows are very short and barely visible.

We can do the same on MNIST, for which we keep our deep autoencoder, and ignore its encoder/decoder structure.

```
corrupted_input = corruptor.corrupt(input)

output = model(corrupted_input)
loss = 0.5 * (output - input).pow(2).sum() / input.size(0)

optimizer.zero_grad()
loss.backward()
optimizer.step()
```

We consider three types of corruptions, that go beyond additive noise:

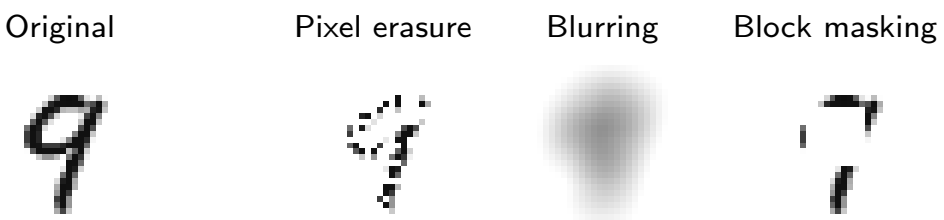

Notes

The architecture of this autoencoder trained on MNIST is the same as in lecture 7.2. "Deep Autoencoders": a series of five convolution layers which narrow the dimension to eight, and a series of five transposed convolutions which increase the size of the maps to the original image size.
The loss is the squared L_2 norm.
We consider three types of corruption:

- pixel erasure: pixels are set to white with a certain probability,
- blurring: the input image is convolved with a Gaussian kernel,
- block masking: a white square is drawn in the middle of the digit.

The strength of the degradation can be modulated by changing respectively

- the probability of erasing a pixel,
- the radius of the Gaussian filter,
- the size of the white patch.

Original

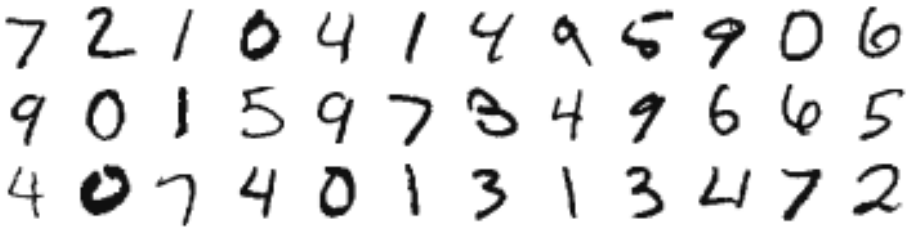

Corrupted ($p = 0.9$)

Reconstructed

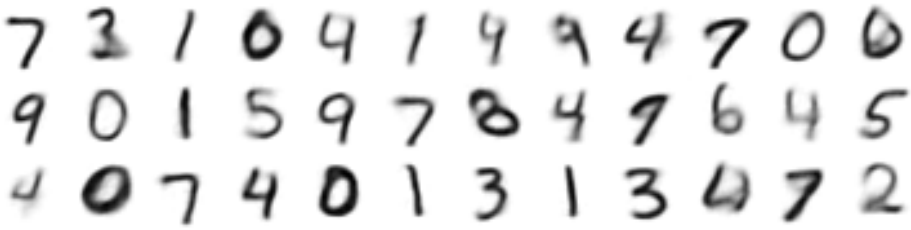

Notes

The three images show:

- some examples of MNIST test samples,
- their corrupted version after erasing the pixels with a probability $p = 0.9$,
- their reconstructed version by the autoencoder.

We observe the same behavior as in the previous course: when a sample is statistically abnormal (e.g. a hole in the line), it is not reconstructed properly (see first digit "0" of bottom row). even though the corrupted digits are barely recognizable, there are not many possibilities to reconstruct them, and the autoencoder learned adequately how to do it.

Original

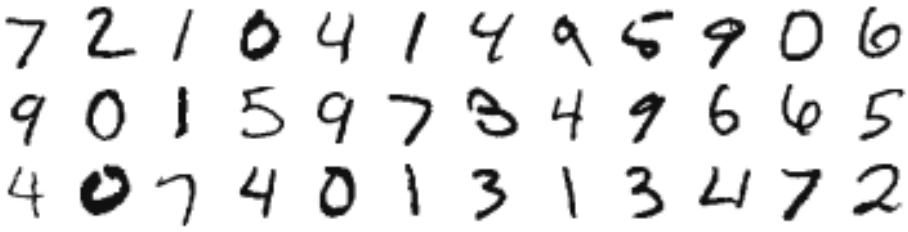

Corrupted ($\sigma = 4$)

Reconstructed

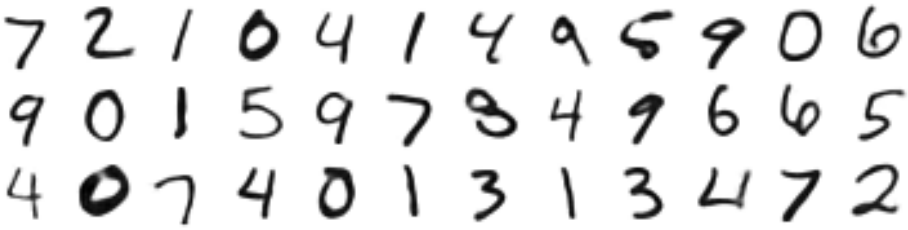

Notes

The three images show:

- some examples of MNIST test samples,
- their corrupted version after blurring the image with a Gaussian filter of size 4 pixels,
- their reconstructed version by the autoencoder.

We can see that blurring is accurately fixed. It is a deterministic linear transformation, and the model simply has to learn the inverse linear operation.

Original

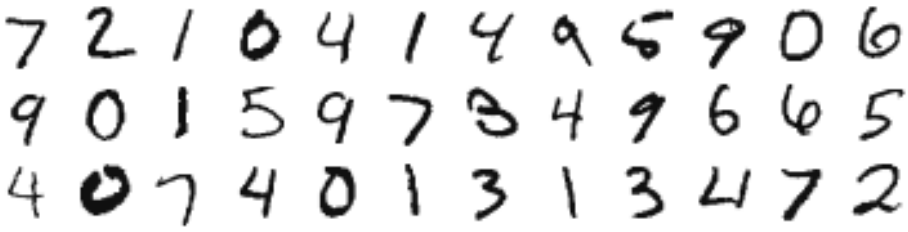

Corrupted (10×10)

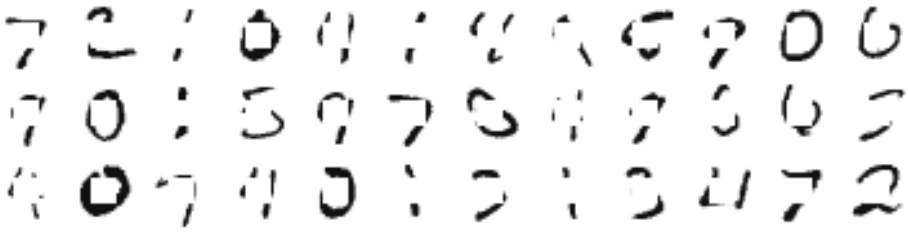

Reconstructed

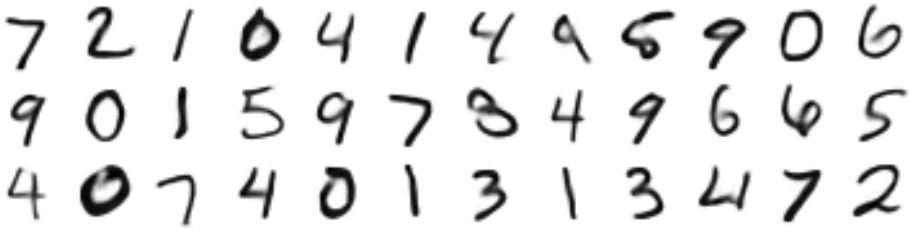

Notes

The images show:

- some examples of MNIST test samples,
- their corrupted version by placing a white mask in the middle of the digit,
- their reconstructed version by the autoencoder

A key weakness of this type of denoising is that the posterior

$$\mu_{X|\tilde{x}}$$

may be non-deterministic, possibly multi-modal.

If we train an autoencoder with the quadratic loss, the best reconstruction is

$$\phi(\tilde{X}) = \mathbb{E}\left[X \,\middle|\, \tilde{X}\right],$$

which may be very unlikely under $\mu_{X|\tilde{x}}$.

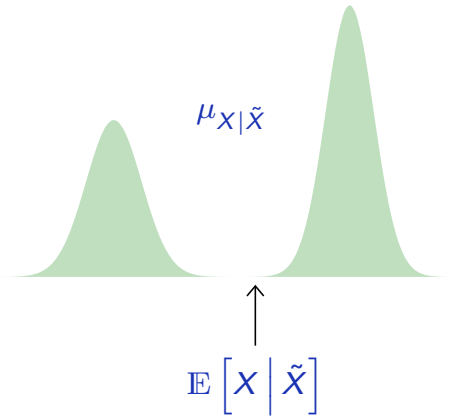

Notes

In the examples of the previous slides, we could observe some blurry parts in the reconstructed digit which can be explained by the fact that the distribution may be multi-modal.
We train the model to generate a deterministic denoised image given a noisy input, and by minimizing the quadratic loss during training, the best output is $\mathbb{E}[X \mid \tilde{X}]$.
However, should the posterior distribution $\mu_{X|\tilde{x}}$ happened to be multi-modal, $\mathbb{E}[X|\tilde{X}]$ may actually be very unlikely under the posterior.

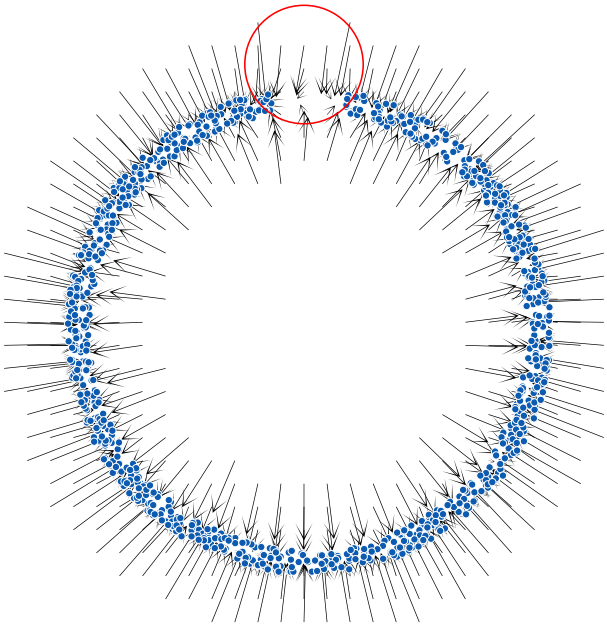

This phenomenon happens here in the area marked with the red circle. Points there can be noisy versions of points originally in either of the two extremities of the open circle, hence minimizing the MSE puts the denoised result in the middle of the opening, even though the density has no mass there.

We can clarify this phenomenon given an $\tilde{x}$ (in blue) by sampling a large number of pairs $(X, \tilde{X})$, keeping only the Xs whose $\tilde{X}$ is very close to $\tilde{x}$, resulting in a sampling of $X|\tilde{X} = \tilde{x}$ (in red), whose mean $\mathbb{E}[X|\tilde{X} = \tilde{x}]$ (in green) minimizes the MSE.

We observe the same phenomenon with very corrupted MNIST digits.

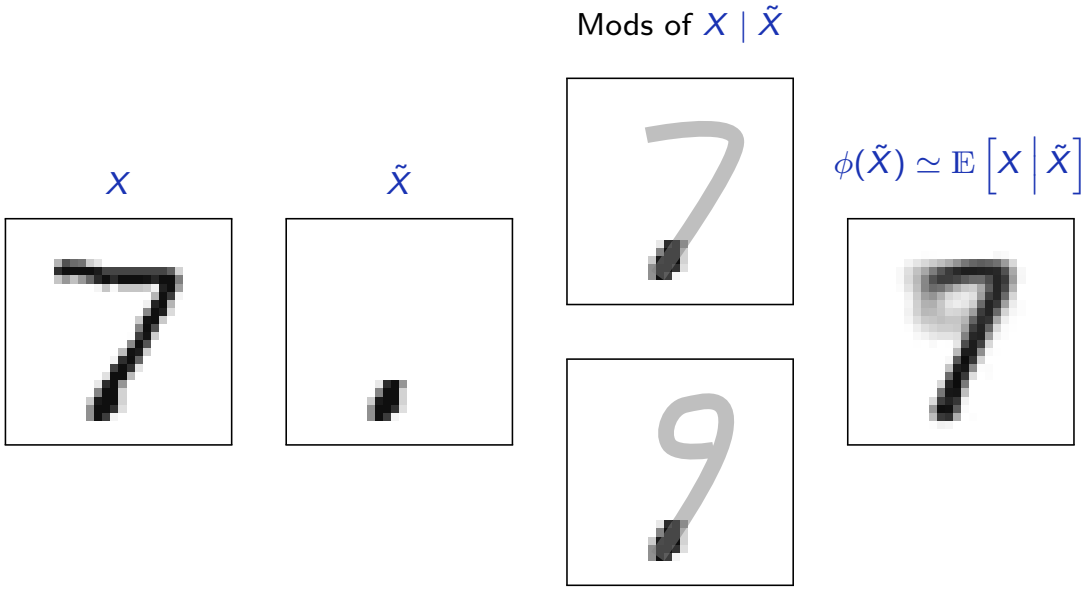

Notes

To illustrate the fact that some reconstructed signals can be improbable under the true distribution, we pick one MNIST digit of the class "7" and degrade it by drawing a large white patch that only keeps the bottom extremity.
Given the piece of information provided by this $\tilde{X}$, the only two possibilities is to have either a "7" or a "9" whose lower part would fit with the remaining fragment. So the reconstructed sample is actually an average under this bi-modal distribution, and looks like a blend of the two digits.

This can be mitigated by using in place of loss a second network that assesses if the output is realistic.

Such methods are called **adversarial** since the second network aims at spotting the mistakes of the first, and the first aims at fooling the second.

It can be combined with a stochastic denoiser that samples an X according to $X \mid \tilde{X}$ instead of computing a deterministic reconstruction.

We will come back to that in lecture 11.1. "Generative Adversarial Networks".

Noise2Noise

Denoising can be achieved without clean samples, if the noise is additive and unbiased. Consider ϵ and δ two unbiased and independent noises. We have

$$\begin{aligned}
&\mathbb{E}\Big[\,\|\phi(X+\epsilon;\theta)-(X+\delta)\|^2\,\Big] \\
&\qquad = \mathbb{E}\Big[\,\|(\phi(X+\epsilon;\theta)-X)-\delta\|^2\,\Big] \\
&\qquad = \mathbb{E}\Big[\,\|\phi(X+\epsilon;\theta)-X\|^2\,\Big] - 2\mathbb{E}\Big[\delta^\top(\phi(X+\epsilon;\theta)-X)\Big] + \mathbb{E}\Big[\|\delta\|^2\Big] \\
&\qquad = \mathbb{E}\Big[\,\|\phi(X+\epsilon;\theta)-X\|^2\,\Big] - 2\underbrace{\mathbb{E}[\delta]^\top}_{=0}\mathbb{E}[\phi(X+\epsilon;\theta)-X] + \mathbb{E}\Big[\|\delta\|^2\Big] \\
&\qquad = \mathbb{E}\Big[\,\|\phi(X+\epsilon;\theta)-X\|^2\,\Big] + \mathbb{E}\Big[\|\delta\|^2\Big].
\end{aligned}$$

Hence

$$\operatorname*{argmin}_\theta \mathbb{E}\Big[\,\|\phi(X+\epsilon;\theta)-(X+\delta)\|^2\,\Big] = \operatorname*{argmin}_\theta \mathbb{E}\Big[\,\|\phi(X+\epsilon;\theta)-X\|^2\,\Big].$$

Using L_1 instead of L_2 estimates the median instead of the mean, and similarly is stable to noise that keeps the median unchanged.

Notes

Here:

- X is the clean signal
- ϵ is some random unbiaised noise, $\mathbb{E}[\epsilon] = 0$,
- δ is another unbiaised noise such that $\mathbb{E}[\delta] = 0$,
- $\phi(X+\epsilon;\theta)$ is the response of the model on the noisy signal with ϵ,
- ϵ and δ are independent and unbiased.

The derivation in this slide shows that minimizing

$$\mathbb{E}\Big[\,\|\phi(X+\epsilon;\theta)-(X+\delta)\|^2\,\Big]$$

is formally equivalent to minimizing

$$\mathbb{E}\Big[\,\|\phi(X+\epsilon;\theta)-X\|^2\,\Big].$$

Hence we can train a model with pairs of noisy samples, if they both correspond to the same unavailable clean samples with different additive, unbiased, and independent noises.

Lehtinen et al. (2018)'s Noise2Noise approach uses this for image restoration, as many existing image generative processes induce an unbiased noise.

> *In many image restoration tasks, the expectation of the corrupted input data is the clean target that we seek to restore. Low-light photography is an example: a long, noise-free exposure is the average of short, independent, noisy exposures.*
>
> *Physically accurate renderings of virtual environments are most often generated through a process known as Monte Carlo path tracing. /.../ The Monte Carlo integrator is constructed such that the intensity of each pixel is the expectation of the random path sampling process, i.e., the sampling noise is zero-mean.*
>
> (Lehtinen et al., 2018)

NAME	N_{out}	FUNCTION
INPUT	n	
ENC_CONV0	48	Convolution 3×3
ENC_CONV1	48	Convolution 3×3
POOL1	48	Maxpool 2×2
ENC_CONV2	48	Convolution 3×3
POOL2	48	Maxpool 2×2
ENC_CONV3	48	Convolution 3×3
POOL3	48	Maxpool 2×2
ENC_CONV4	48	Convolution 3×3
POOL4	48	Maxpool 2×2
ENC_CONV5	48	Convolution 3×3
POOL5	48	Maxpool 2×2
ENC_CONV6	48	Convolution 3×3
UPSAMPLE5	48	Upsample 2×2
CONCAT5	96	Concatenate output of POOL4
DEC_CONV5A	96	Convolution 3×3
DEC_CONV5B	96	Convolution 3×3
UPSAMPLE4	96	Upsample 2×2
CONCAT4	144	Concatenate output of POOL3
DEC_CONV4A	96	Convolution 3×3
DEC_CONV4B	96	Convolution 3×3
UPSAMPLE3	96	Upsample 2×2
CONCAT3	144	Concatenate output of POOL2
DEC_CONV3A	96	Convolution 3×3
DEC_CONV3B	96	Convolution 3×3
UPSAMPLE2	96	Upsample 2×2
CONCAT2	144	Concatenate output of POOL1
DEC_CONV2A	96	Convolution 3×3
DEC_CONV2B	96	Convolution 3×3
UPSAMPLE1	96	Upsample 2×2
CONCAT1	$96+n$	Concatenate INPUT
DEC_CONV1A	64	Convolution 3×3
DEC_CONV1B	32	Convolution 3×3
DEV_CONV1C	m	Convolution 3×3, linear act.

(Lehtinen et al., 2018)

Input, 8 spp	L_2 with $\hat{x}, \hat{y}$	L_2 with $T(\hat{x}), \hat{y}$	L_2 with $T(\hat{x}), T(\hat{y})$	L_{HDR} with $\hat{x}, \hat{y}$	L_{HDR} with $T(\hat{x}), \hat{y}$	Reference, 32k spp
11.32 dB	25.46 dB	25.39 dB	15.50 dB	29.05 dB	30.09 dB	PSNR

Figure 6. Comparison of various loss functions for training a Monte Carlo denoiser with noisy target images rendered at 8 samples per pixel (spp). In this high-dynamic range setting, our custom relative loss L_{HDR} is clearly superior to L_2. Applying a non-linear tone map to the inputs is beneficial, while applying it to the target images skews the distribution of noise and leads to wrong, visibly too dark results.

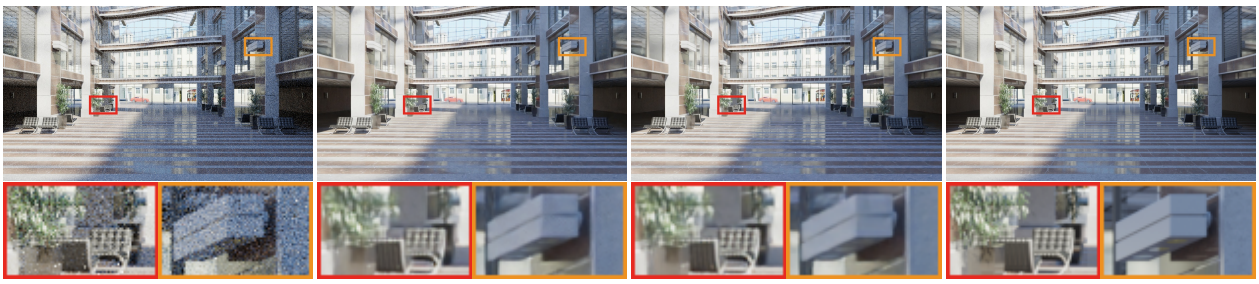

(a) Input (64 spp), 23.93 dB (b) Noisy targets, 32.42 dB (c) Clean targets, 32.95 dB (d) Reference (131k spp)

Figure 7. Denoising a Monte Carlo rendered image. (a) Image rendered with 64 samples per pixel. (b) Denoised 64 spp input, trained using 64 spp targets. (c) Same as previous, but trained on clean targets. (d) Reference image rendered with 131 072 samples per pixel. PSNR values refer to the images shown here, see text for averages over the entire validation set.

(Lehtinen et al., 2018)

Notes

On both figures: the leftmost picture is the noisy CGI input generated with a small number of sample per pixel (8 on figure 6, and 64 on figure 7) , the second from the left is the denoised version obtained with the Noise2Noise method, and the rightmost one the reference CGI, generated with a large number of samples per pixel ($32k$ on figure 6, and $131k$ on figure 7).

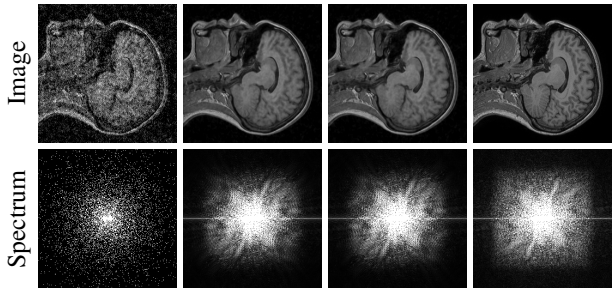

(a) Input 18.93 dB (b) Noisy trg. 29.77 dB (c) Clean trg. 29.81 dB (d) Reference

Figure 9. MRI reconstruction example. (a) Input image with only 10% of spectrum samples retained and scaled by $1/p$. (b) Reconstruction by a network trained with noisy target images similar to the input image. (c) Same as previous, but training done with clean target images similar to the reference image. (d) Original, uncorrupted image. PSNR values refer to the images shown here, see text for averages over the entire validation set.

(Lehtinen et al., 2018)

Notes

Noise2Noise can be used for magnetic resonance imaging reconstruction. MRI scans can be undersampled because this technology is very slow, and may be difficult to obtain with dynamic subjects.

Super-resolution

A special case of denoising is to increase an image resolution. We use an encoder/decoder whose encoder's input is smaller than the decoder's output.

Encoder

Tensor sizes / operations	
$1 \times 14 \times 14$	
`nn.Conv2d(1, 32, kernel_size=5, stride=1)`	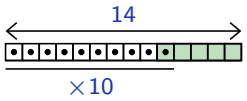
$32 \times 10 \times 10$	
`nn.Conv2d(32, 32, kernel_size=5, stride=1)`	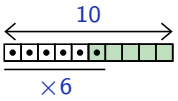
$32 \times 6 \times 6$	
`nn.Conv2d(32, 32, kernel_size=4, stride=1)`	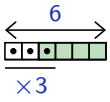
$32 \times 3 \times 3$	
`nn.Conv2d(32, 32, kernel_size=3, stride=1)`	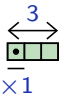
$32 \times 1 \times 1$	

Notes

Increasing the resolution of an image can be useful for high resolution TV, because in many situations, the input signal is of low quality compared to the screen resolution (old TV series, etc.)
Increasing the image with standard bilinear interpolation yields extremely unpleasant artifacts. We can instead train a deep network to learn how to perform the up-scaling based on the content of the signal: regenerating high-frequency patterns when necessary, keeping the edges sharp, etc.
To illustrate how such a upsampler can be trained, we use the MNIST dataset with input images down-sampled by a factor 2: the input images are of size $1 \times 14 \times 14$ instead of $1 \times 28 \times 28$. The encoder reduces the size of the signal from $1 \times 14 \times 14$ down to $32 \times 1 \times 1$. And we then uses a decoder to upsample the signal up to $1 \times 28 \times 28$.

```
MNISTUpscaler(
  (encoder): Sequential(
    (0): Conv2d(1, 32, kernel_size=(5, 5), stride=(1, 1))
    (1): ReLU(inplace=True)
    (2): Conv2d(32, 32, kernel_size=(5, 5), stride=(1, 1))
    (3): ReLU(inplace=True)
    (4): Conv2d(32, 32, kernel_size=(4, 4), stride=(1, 1))
    (5): ReLU(inplace=True)
    (6): Conv2d(32, 32, kernel_size=(3, 3), stride=(1, 1))
  )
  (decoder): Sequential(
    (0): ConvTranspose2d(32, 32, kernel_size=(4, 4), stride=(1, 1))
    (1): ReLU(inplace=True)
    (2): ConvTranspose2d(32, 32, kernel_size=(3, 3), stride=(2, 2))
    (3): ReLU(inplace=True)
    (4): ConvTranspose2d(32, 32, kernel_size=(4, 4), stride=(2, 2))
    (5): ReLU(inplace=True)
    (6): ConvTranspose2d(32, 32, kernel_size=(5, 5), stride=(1, 1))
    (7): ReLU(inplace=True)
    (8): ConvTranspose2d(32, 1, kernel_size=(5, 5), stride=(1, 1))
  )
)
```

Notes

This model has a structure very similar to the autoencoder of lecture 7.2. "Deep Autoencoders".

```
for original in train_input.split(batch_size):
    input = F.avg_pool2d(original, kernel_size = 2)
    output = model(input)
    loss = (output - original).pow(2).sum() / output.size(0)

    optimizer.zero_grad()
    loss.backward()
    optimizer.step()
```

Notes

The training goes exactly as usual:

- the image size is reduced by a factor of 2 with an average pooling,
- we use a quadratic loss between the output of the autoencoder and the original full resolution image.

Original

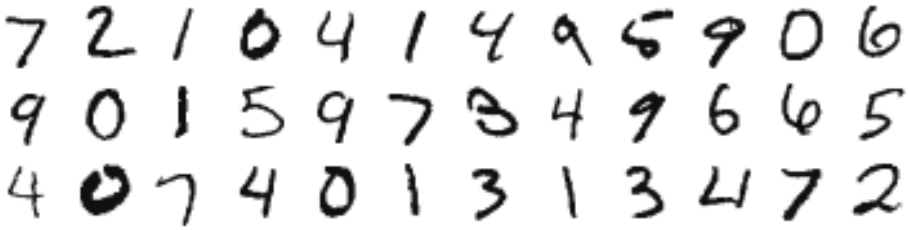

Input

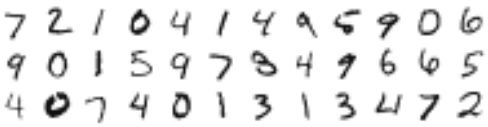

Bilinear interpolation

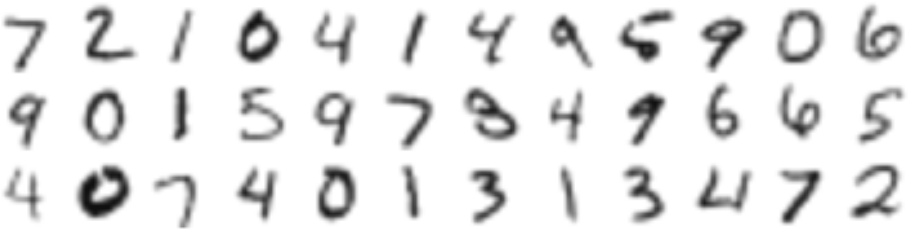

Notes

We show here the results of upsampling with a standard bilinear interpolation:

- The top images are the original $1 \times 28 \times 28$ test MNIST images,
- the middle images are the input images of size $1 \times 14 \times 14$,
- the bottom images are the result with the bilinear upsampling which performs local interpolation. We can easily spot the blurring of such a method.

Original

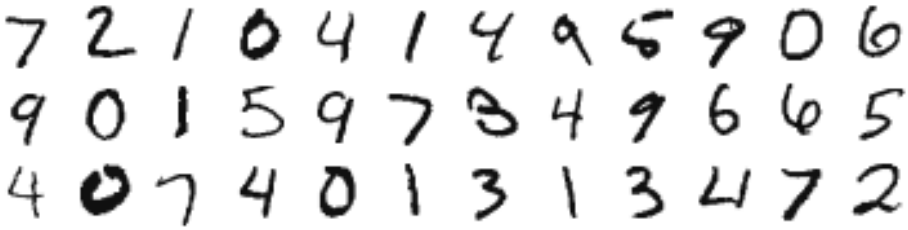

Input

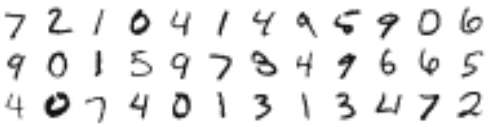

Autoencoder output

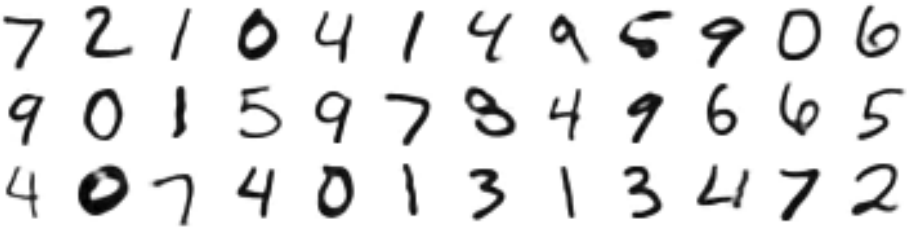

Notes

We show here the results obtained with our deep up-sampler.

- The top images are the original $1 \times 28 \times 28$ test MNIST images,
- the middle images are the input images of size $1 \times 14 \times 14$,
- the bottom images are the output of the up-sampler. The digit are sharper and more realistic, although we can observe some blurriness effects at the border of the digit. This is due to the same effect as before: the autoencoder produces the conditional expectation and not the most likely sample.

Lim et al. (2017) use two different resnets.

	EDSR	MDSR
Nb blocks	32	80
Channels	256	64
Nb parameters	43M	8M

img034 from Urban100 [10]

HR (PSNR / SSIM)

Bicubic (21.41 dB / 0.4810)

A+ [27] (22.21 dB / 0.5408)

SRCNN [4] (22.33 dB / 0.5461)

VDSR [11] (22.62 dB / 0.5657)

SRResNet [14] (23.14 dB / 0.5891)

EDSR+ (Ours) (23.48 dB / 0.6048)

MDSR+ (Ours) (23.46 dB / 0.6039)

(Lim et al., 2017)

Notes

These results is an application of upsampling autoencoders on real images where

- the "HR" image is the original high resolution image,
- the "bicubic" is an interpolation similar to bilinear interpolation but at a higher degree,
- the deep learning based method are able to produced sharper edges consistent with the local context around pixels.

Lim et al. (2017) use two different resnets.

	EDSR	MDSR
Nb blocks	32	80
Channels	256	64
Nb parameters	43M	8M

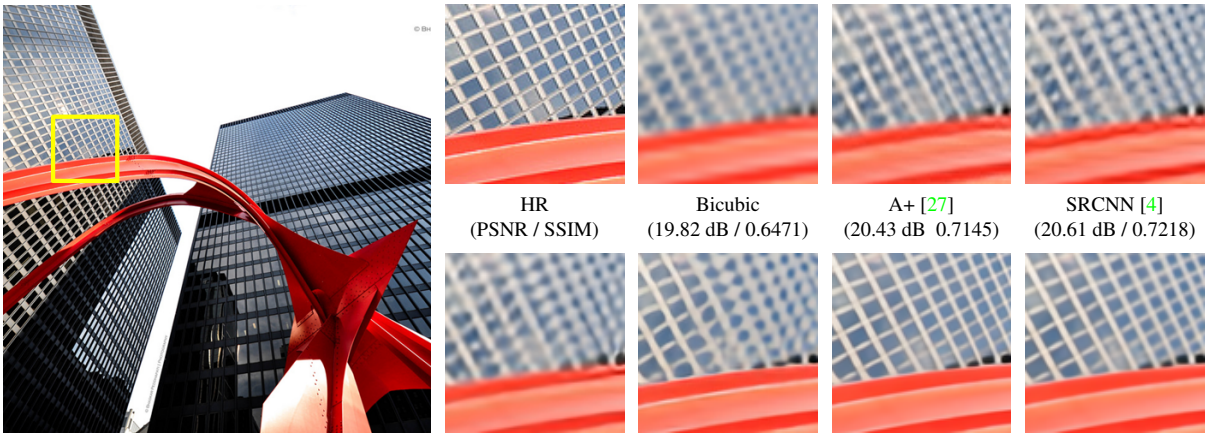

(Lim et al., 2017)

Notes

These results is an application of upsampling autoencoders on real images where

- the "HR" image is the original high resolution image,
- the "bicubic" is an interpolation similar to bilinear interpolation but at a higher degree,
- the deep learning based method are able to produced sharper edges consistent with the local context around pixels.

Lim et al. (2017) use two different resnets.

	EDSR	MDSR
Nb blocks	32	80
Channels	256	64
Nb parameters	43M	8M

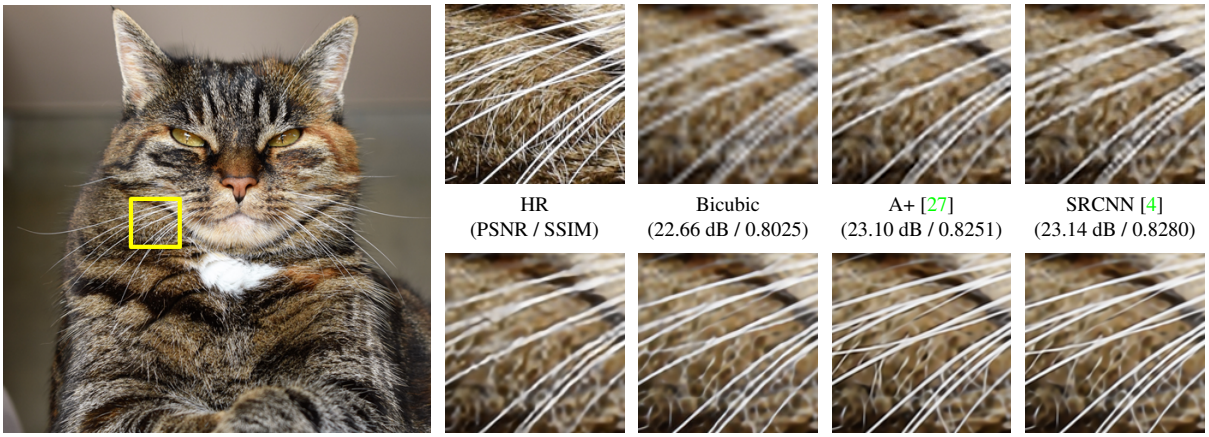

(Lim et al., 2017)

Notes

These results is an application of upsampling autoencoders on real images where

- the "HR" image is the original high resolution image,
- the "bicubic" is an interpolation similar to bilinear interpolation but at a higher degree,
- the deep learning based method are able to produced sharper edges consistent with the local context around pixels.

Autoencoders as self-training

Vincent et al. (2010) interpret training the autoencoder as maximizing the mutual information between the input and the latent states.

Let X be a sample, $Z = f(X;\theta)$ its latent representation, and $q(x,z)$ the distribution of (X,Z).

We have

$$\operatorname*{argmax}_{\theta} \mathbb{I}(X;Z) = \operatorname*{argmax}_{\theta} \mathbb{E}_{q(X,Z)}\Big[\log q(X \mid Z)\Big].$$

However, there is no expression of $q(X \mid Z)$ in any reasonable setup.

Notes

One avenue of research has been to train deep networks by pre-training them using unlabeled data, which can often be obtained in large quantities.
The encoder f of an autoencoder seems to be a good pre-trained model since it "discovered" a low-dimension representation of the data the capture its structure.

However, for any distribution p we have

$$\mathbb{E}_{q(X,Z)}\Big[\log q(X \mid Z)\Big] \geq \mathbb{E}_{q(X,Z)}\Big[\log p(X \mid Z)\Big].$$

So we can in particular try to find a "good p", so that the right term is a good approximation of the left one.

If we consider the following model for p

$$p(\cdot \mid Z = z) = \mathcal{N}(g(z;\eta), \sigma)$$

where g is deterministic and σ fixed, we get

$$\mathbb{E}_{q(X,Z)}\Big[\log p(X \mid Z)\Big] = -\frac{1}{2\sigma^2}\mathbb{E}_{q(X,Z)}\left[\|X - g(f(X;\theta);\eta)\|^2\right] + k.$$

If optimizing η makes the bound tight, the final loss is the reconstruction error

$$\operatorname*{argmax}_{\theta} \mathbb{I}(X;Z) \simeq \operatorname*{argmin}_{\theta}\left(\min_{\eta} \frac{1}{N}\sum_{n=1}^{N}\|x_n - g(f(x_n;\theta);\eta)\|^2\right).$$

This abstract view of the encoder as "maximizing information" justifies its use to build generic encoding layers.

Notes

The problem boils down to finding θ such that there exists a good decoder: if θ is such that we can indeed reconstruct the original signal, then no information was lost.
Under a Gaussian model, $\mathcal{N}(g(z;\eta), \sigma)$ we have

$$p(X \mid Z) = \frac{1}{\sqrt{2\pi\sigma^2}} \exp\left(-\frac{\|X - g(z;\eta)\|^2}{2\sigma^2}\right)$$

hence

$$\log p(X \mid Z) = -\frac{1}{2\sigma^2}\|X - g(z;\eta)\|^2 + k,$$

where $k = -\frac{1}{2}\log 2\pi\sigma^2$.

In the perspective of building a good feature representation, just retaining information is not enough, otherwise the identity would be a good choice.

In their work, Vincent et al. consider a denoising auto-encoder, which makes the model retain information about structures beyond local noise.

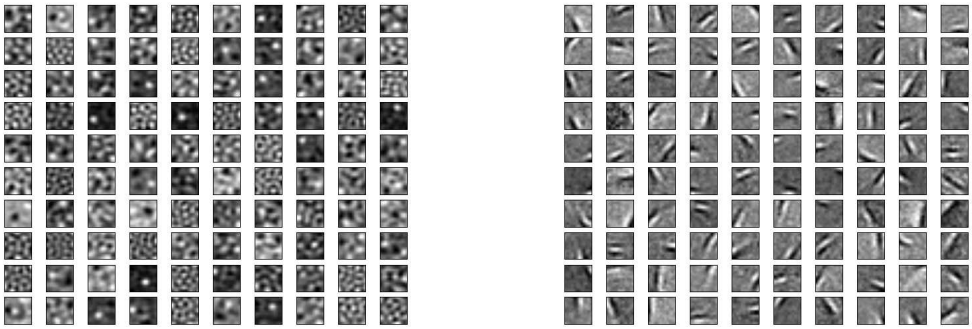

Figure 6: Weight decay vs. Gaussian noise. We show typical filters learnt from natural image patches in the over-complete case (200 hidden units). *Left:* regular autoencoder with weight decay. We tried a wide range of weight-decay values and learning rates: filters never appeared to capture a more interesting structure than what is shown here. Note that some local blob detectors are recovered compared to using no weight decay at all (Figure 5 right). *Right:* a denoising autoencoder with additive Gaussian noise ($\sigma = 0.5$) learns Gabor-like local oriented edge detectors. Clearly the filters learnt are qualitatively very different in the two cases.

(Vincent et al., 2010)

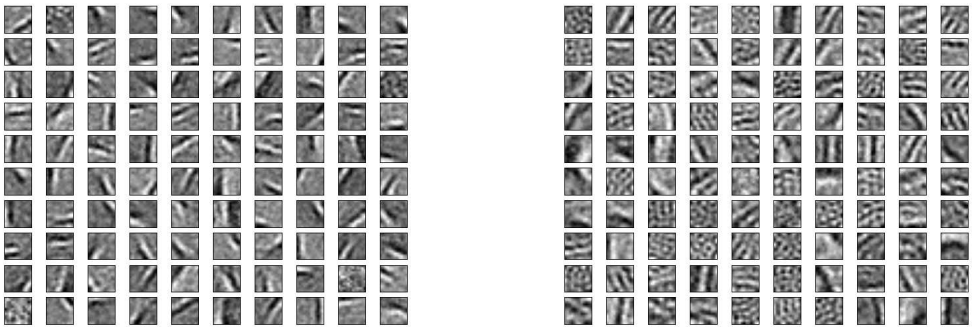

Figure 7: Filters obtained on natural image patches by denoising autoencoders using other noise types. *Left:* with 10% salt-and-pepper noise, we obtain oriented Gabor-like filters. They appear slightly less localized than when using Gaussian noise (contrast with Figure 6 right). *Right:* with 55% zero-masking noise we obtain filters that look like oriented gratings. For the three considered noise types, denoising training appears to learn filters that capture meaningful natural image statistics structure.

(Vincent et al., 2010)

Vincent et al. build deep MLPs whose layers are initialized successively as encoders trained within a noisy autoencoder.

A final classifying layer is added and the full structure can be fine-tuned.

This approach, and others in the same spirit (Hinton et al., 2006), were seen as strategies to complement gradient-descent for building deep nets.

Notes

These techniques of using autoencoders to pre-train deep network predates more recent techniques such as careful initialization and rectifiers which made them less needed.

Data Set	SVM_{rbf}	DBN-1	SAE-3	DBN-3	SDAE-3 (ν)
MNIST	**1.40**±0.23	**1.21**±0.21	**1.40**±0.23	**1.24**±0.22	**1.28**±0.22 (25%)
basic	**3.03**±0.15	3.94±0.17	3.46±0.16	3.11±0.15	**2.84**±0.15 (10%)
rot	11.11±0.28	14.69±0.31	10.30±0.27	10.30±0.27	**9.53**±0.26 (25%)
bg-rand	14.58±0.31	9.80±0.26	11.28±0.28	**6.73**±0.22	10.30±0.27 (40%)
bg-img	22.61±0.37	**16.15**±0.32	23.00±0.37	**16.31**±0.32	**16.68**±0.33 (25%)
bg-img-rot	55.18±0.44	52.21±0.44	51.93±0.44	47.39±0.44	**43.76**±0.43 (25%)
rect	**2.15**±0.13	4.71±0.19	2.41±0.13	2.60±0.14	**1.99**±0.12 (10%)
rect-img	24.04±0.37	23.69±0.37	24.05±0.37	22.50±0.37	**21.59**±0.36 (25%)
convex	19.13±0.34	19.92±0.35	**18.41**±0.34	**18.63**±0.34	**19.06**±0.34 (10%)
tzanetakis	**14.41**±2.18	18.07±1.31	**16.15**±1.95	18.38±1.64	**16.02**±1.04(0.05)

(Vincent et al., 2010)

References

G. E. Hinton, S. Osindero, and Y.-W. Teh. **A fast learning algorithm for deep belief nets**. Neural Computation, 18(7):1527–1554, July 2006.

J. Lehtinen, J. Munkberg, J. Hasselgren, S. Laine, T. Karras, M. Aittala, and T. Aila. **Noise2noise: Learning image restoration without clean data**. CoRR, abs/1803.04189, 2018.

B. Lim, S. Son, H. Kim, S. Nah, and K. Lee. **Enhanced deep residual networks for single image super-resolution**. CoRR, abs/1707.02921v1, 2017.

P. Vincent, H. Larochelle, I. Lajoie, Y. Bengio, and P.-A. Manzagol. **Stacked denoising autoencoders: Learning useful representations in a deep network with a local denoising criterion**. Journal of Machine Learning Research (JMLR), 11:3371–3408, 2010.